



ISSN ONLINE: 2447-0228



DIRECTIONAL UWB ANTENNA FOR BREAST CANCER DETECTION

Olayiwola Charles Adesoba*¹

¹ Federal University of Technology: Akure, Ondo, Nigeria.

¹ <http://orcid.org/0009-0007-1238-2287> 

Email: *ocadesoba@futa.edu.ng

ARTICLE INFO

Article History

Received: May 24th, 2023
Accepted: June 27th, 2023
Published: June 30th, 2023

Keywords:

Ultra-wideband (UWB),
Return loss,
Radiation Pattern,
Impedance Bandwidth,
Anechoic chamber.

ABSTRACT

A simple and compact ultra-wideband (UWB) antenna is presented. The proposed antenna is fabricated on a FR4 printed circuit board of a rectangular aperture. Two models of the proposed antenna are presented and the difference between the two models is the addition of an additional ground plane, added so as to obtain a uni-directional radiation pattern. The antenna consists of two ground planes, one serving as a reflector and a T-shaped excitation stub. The fundamental characteristics of the antenna such as impedance bandwidth, return loss and radiation pattern are obtained. The antenna is successfully designed, optimised and measured. The result shows that the proposed antenna achieves an impedance bandwidth of 4.2-10GHz with a return loss greater than 10dB, except in the band of 5.8-6.4GHz and 10-10.6GHz. Generally, the input impedance is not well matched at lower frequencies of 3.1-4GHz from both simulation and measured results. The measurement of the radiation pattern is performed in the anechoic chamber at frequencies of 3GHz, 4GHz, 5GHz and 6GHz. The designed antenna has a simple structure and compact size of $13 \times 23 \text{ mm}^2$.



Copyright ©2023 by authors and Galileo Institute of Technology and Education of the Amazon (ITEGAM). This work is licensed under the Creative Commons Attribution International License (CC BY 4.0).

I. INTRODUCTION

Breast cancer is the most common non-skin related malignancy and the second leading cause of cancer death among women in the world [1]. The rate of mortality of women with cancer was very high about fifty years ago as there was no established method for early stage detection. Thousands of women die from the disease every year. Early detection is the best hope for reducing the serious toll of this disease until researchers uncovers a way to prevent breast cancer or cure the women with the disease.

Technological advancements has made the situation change, the first suggested technology for breast cancer detection was the X-ray imaging. It was proved to be the most effective tool for the early detection of breast cancer, though it has its own limitations. The major limitation is false positive results showing signs of cancer that are ruled out when further testing is carried out, this technology cannot actually detect which cancer would be harmful or less harmful, so therefore, all signs of cancer detected would be treated as malicious. This restraint is known as over-diagnosis [2]. Over the past decades, the investment in breast cancer research including early detection has increased significantly. Improved and new technologies are rapidly emerging

and providing hope of early detection. The limitations of the use of X-ray mammography for breast cancer detection motivated the search for a better alternative and this alternative is the microwave imaging.

Ultra-wideband (UWB) is an attractive emerging technology for both wireless communications and microwave imaging. The Ultra-wide band technology is a technology completely based upon the radio waves for the sake of communication among small distances but at a very high rate or speed.

In 1980s, the Industrial Scientific Medicine (ISM) band for unlicensed wideband communication use was allocated by the Federal Communication Commission (FCC). A bandwidth of 7.5GHz, from 3.1-10.6GHz was allocated by the FCC to Ultra-wideband (UWB) applications [3]. Any signal that occupies at least 500MHz spectrum can be used in UWB systems; this is in accordance with the FCC's ruling which makes UWB not restricted to impulse radio any longer, it also applies to any technology that uses 500MHz spectrum and complies with all other requirements for UWB.

The major problem in UWB antenna design is how to obtain a large impedance bandwidth while maintaining a high radiation

performance. A bandwidth higher than 100% of the centre frequency is required in an Ultra-wideband system; therefore, an impedance matching is required throughout the bandwidth in the case of this project. The power loss due to reflections must be minimized since the transmission power is very low and this is the major reason why a miniaturised and compact antenna is needed.

Another problem to be addressed in this project is how to reduce the undesirable side effects of the image received and also ensure the design of the directional UWB antenna covers an immensely wide band, 3.1-10.6GHz for indoor and handheld UWB applications, have an electrical small size and able to handle a moderate impedance match over the band for high proficiency.

My experiment was implemented using a microwave design software – CST microwave studio which was capable of transmitting or receiving UWB signals and can achieve a directional radiation pattern and a sufficient impedance bandwidth.

The rest of this paper is organized as follows: Section II provides a basic background to UWB Antennas together with published studies on how UWB Antennas are being developed and implemented. In section III, I present the methodology for the study as well as the simulation parameters. In section IV, I present and

discuss the results obtained from the study, and finally, in section V, I conclude the study.

II. THEORETICAL REFERENCE

II.1 BACKGROUND STUDY AND RELATED WORKS

The present literature of directional UWB antenna is fast increasing in terms of development as a number of techniques are proposed for the improvement on microwave imaging. There are several antennas already designed for this purpose, like the compact coplanar waveguide-fed Ultra-wideband monopole-like slot antenna, low-profile directional UWB antenna for see-through-wall imaging applications, a miniaturized directional UWB antenna and many more.

[4] proposed a compact coplanar waveguide-fed UWB monopole-like slot antenna which comprises of a monopole-like slot and a CPW fork shaped feeding structure which is etched onto a FR4 Printed Circuit Board with a dimension of $26\text{mm} \times 29\text{mm} \times 18\text{mm}$ as shown in Figure 1.

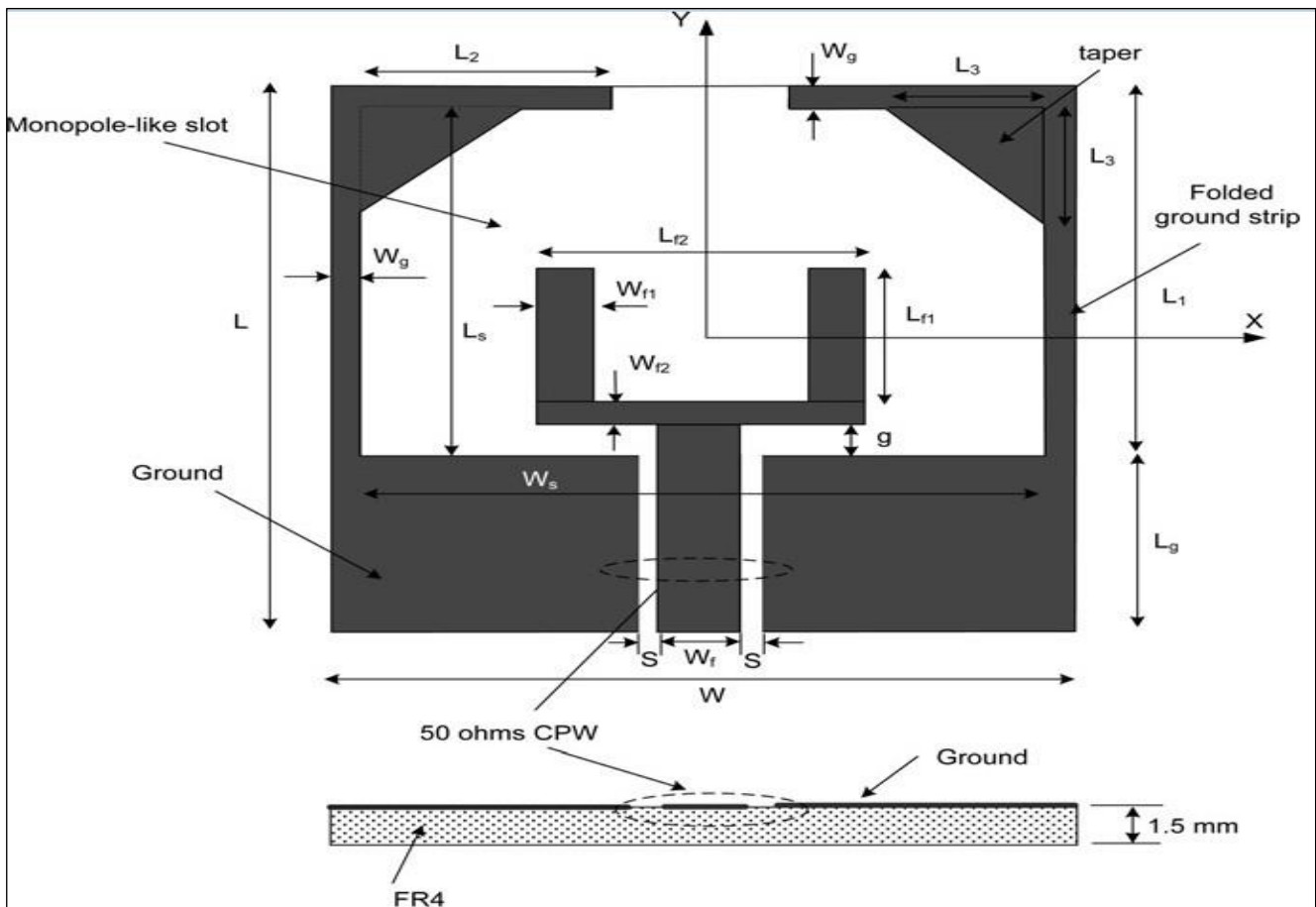


Figure 1: Geometry and Configuration of the Proposed Monopole-like Slot Antenna.

Source: [4].

Both the slot and the fork-shaped feeding structure were printed on the same side of a piece of FR4 substrate with a thickness of 1.5mm, a loss tangent of $\tan \delta = 0.02$ and a relative dielectric constant of 4.4 positioned symmetrically with respect to the centreline of the slot. The use of a fork-shaped feeding structure is to obtain more efficient coupling between the feeding structure and the slot, which is significant for the achievement of an improved bandwidth of the slot antenna [5]. The radiation patterns

of the antenna were measured at lower and higher frequencies. A good omni-directional radiation pattern in the H-plane was achieved at lower frequencies while a bi-directional pattern was obtained at higher frequencies due to the comparison of the spacing of the fork shaped stubs to the wavelength. The slot follows the shape of a corresponding planar monopole antenna. The ground plane of the monopole-like slot antenna is not closed compared to

the traditional wide slot antenna. The slot is enclosed by two ground layers with small breadth which makes the antenna small.

The proposed antenna was simulated using the CST Microwave studio based on Finite Integration Technique (FIT). The antenna was measured using HP8510 vector analyser and Orbit MiDAS 4.0 far-field antenna measurement system in a full

anechoic chamber. The simulation and experiment showed that the proposed antenna achieves good impedance matching, stable radiation patterns, and consistent gain. A good accordance was established between the simulated and measured return loss, a bandwidth of 2.7-12.4GHz and a return loss of -10dB was achieved likewise a good accordance in terms of gain ($\theta = 0^\circ, \phi = 0^\circ$).

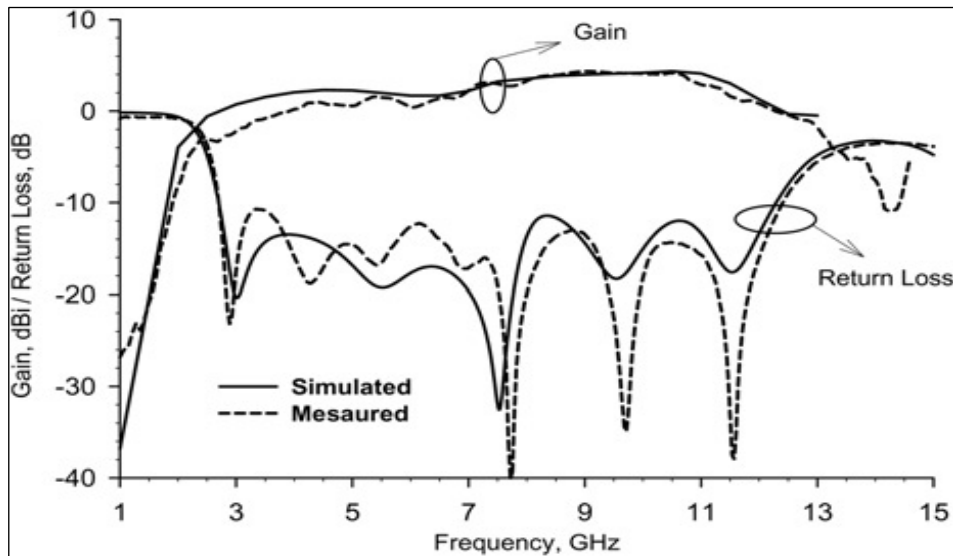


Figure 2: Simulated and Measured Return Loss as well as Gain at ($\theta = 0^\circ, \phi = 0^\circ$). Source: [4].

In a parametric study carried out by [4-6], the impedance bandwidth of -10dB return loss was examined. It was found out that the width of the slot, W_s determines the operating band of the antenna and that the lower frequency edge of the operating bandwidth is the most easily affected to the length of the horizontal folded ground trips, L_2 , whereas the higher frequency edge depends on the dimensions of the fork-shaped feeding stubs, L_{f1} and L_{f2} . The remaining parameters do not show significant effect on the impedance bandwidth but can be made effective to improve the impedance matching.

The authors in [6] presented a compact-size planar antenna with UWB bandwidth and directional pattern as shown in Figure 3. Three types of directional UWB Antennas were analysed. The antenna was fabricated on a Printed Circuit Board (PCB). In their design, there is a circular path on one side of the PCB and a slot-embedded ground plane with a fork-shaped feeding stub in the slot on the other side of the PCB. A reflector which was placed below the antenna was used to achieve a directional radiation pattern. Their aim was to examine novel designs of low cost and small antennas suitable for UWB through the wall imaging radar.

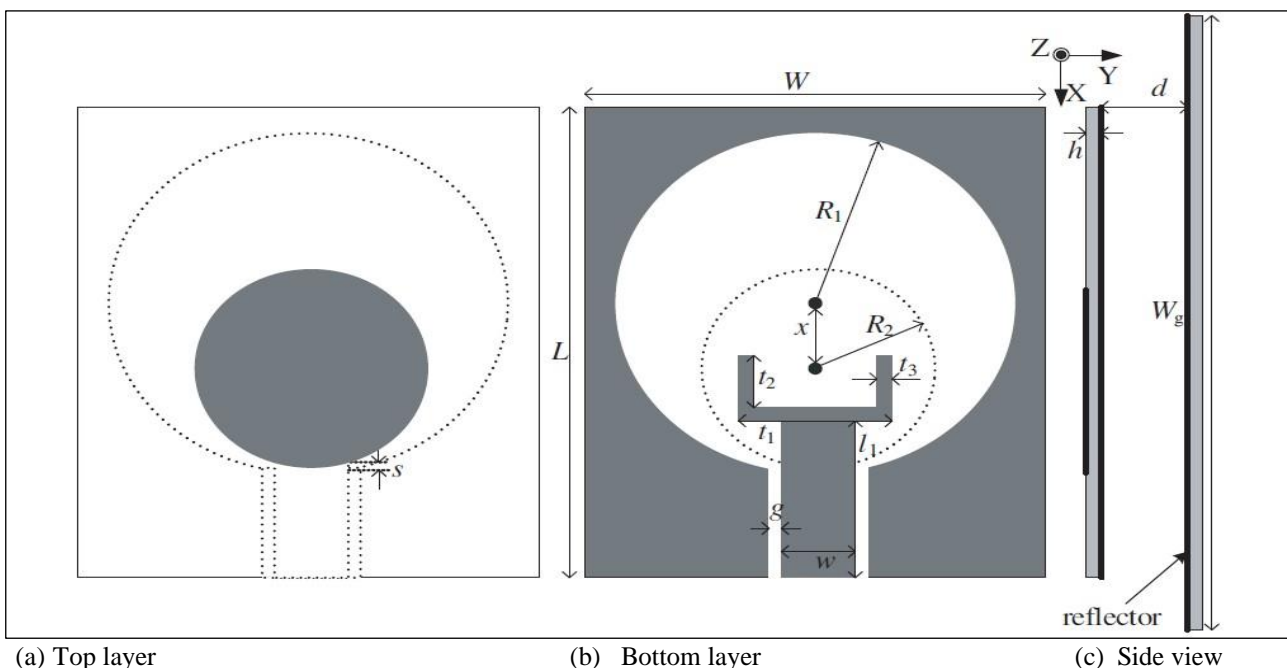


Figure 3: Configuration of the Low Profile Directional UWB Antenna. Source: [6].

Major challenges of the UWB antenna design was further analysed which are impedance matching, directional patterns, low distortion of pulses, compact size, low cost and high front to back ratio for the rejection of false alarms from the movement of the user holding the device. The main problem of the directional UWB antenna with a reflector is the thickness of the antenna, as the reflector usually needs to be located at a distance of a quarter wavelengths from the antenna, though, this would unfortunately affect the radiation efficiency and impedance matching of the antenna especially at lower frequencies band due to the small electrical distance to the reflector [7].

A new low profile antenna configuration was proposed so as to reduce the antenna's thickness, two reference antennas with directional patterns are used and comparison was carried out on the results [6], [7]. There are 2 major ways of increasing the bandwidth of a slot antenna, the first one is the manipulation of the field distribution in the slot with a circular patch and the second way is the use of a circular slot and a fork-like stub for excitation [8].

The first way is illustrated in Figure 4 which was used as the Reference Antenna 1 and the second way was used as the Reference Antenna 2, this is shown in Figure 6.

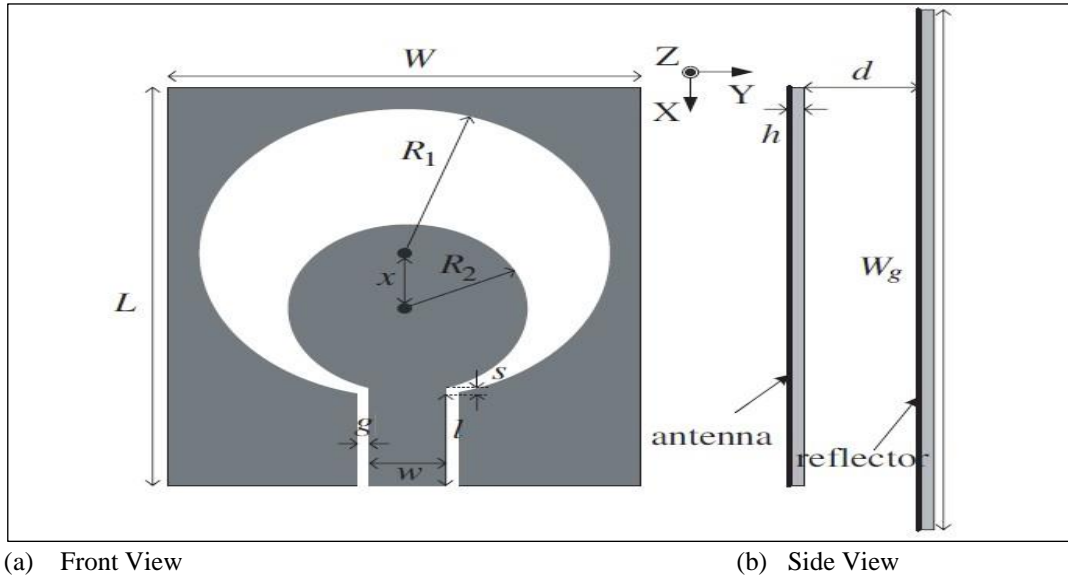


Figure 4: Configuration of UWB Reference Antenna with Reflector (Reference Antenna 1). Source: [6].

The reference antenna 1 above makes use of a circular patch to manipulate the field distribution in the slot. The radiation pattern of this antenna is omni-directional in H-plane and bi-directional in E-plane. The reflector is added so as to achieve the directional patterns of the antenna. In this paper, the reflection coefficient was simulated in terms of the distance d between the antenna and the reflector and was plotted in a graph against the frequency. The result showed that the impedance matching of the antenna has been

greatly affected by the reflector mainly at lowest frequencies compared to the original antenna without a reflector.

The outcome of the reflection coefficients at various distances between the reflector and the antenna is shown in Figure 5. It can be deduced from the Figure that at the lowest frequency for $S_{11} < -10\text{dB}$ shifts from 6.7GHz to 5.8GHz when the distance increases from 12mm to 16mm, therefore, bringing about a huge antenna.

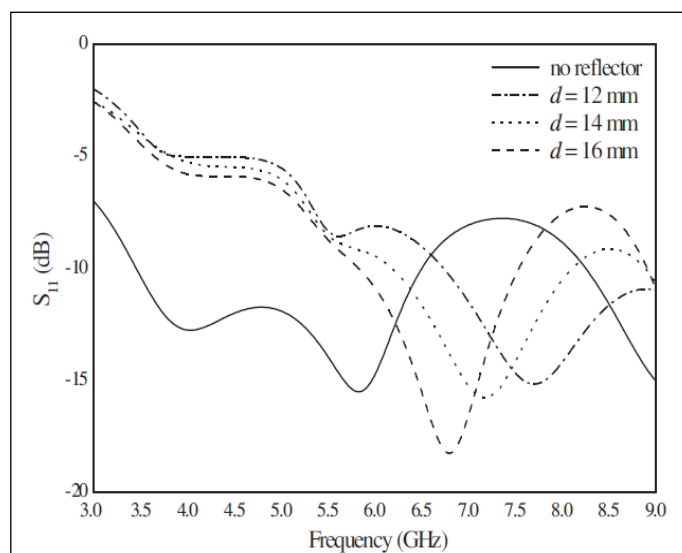


Figure 5: Simulated Return Losses in terms of d compared to the Case of no Reflector. Source: [6].

The substrate used is the Duroid 5880 which has a dielectric constant of 2.2 and a thickness of 1.575mm. The frequency band of the designed UWB Antenna is from 4.5-8.5GHz. This type of antenna described is a Coplanar Waveguide (CPW) fed UWB slot

antenna. The maximum value of S shouldn't be larger than the substrate thickness h [9]. Authors in [9] states that the slot aperture relatively depends on the lowest frequency.

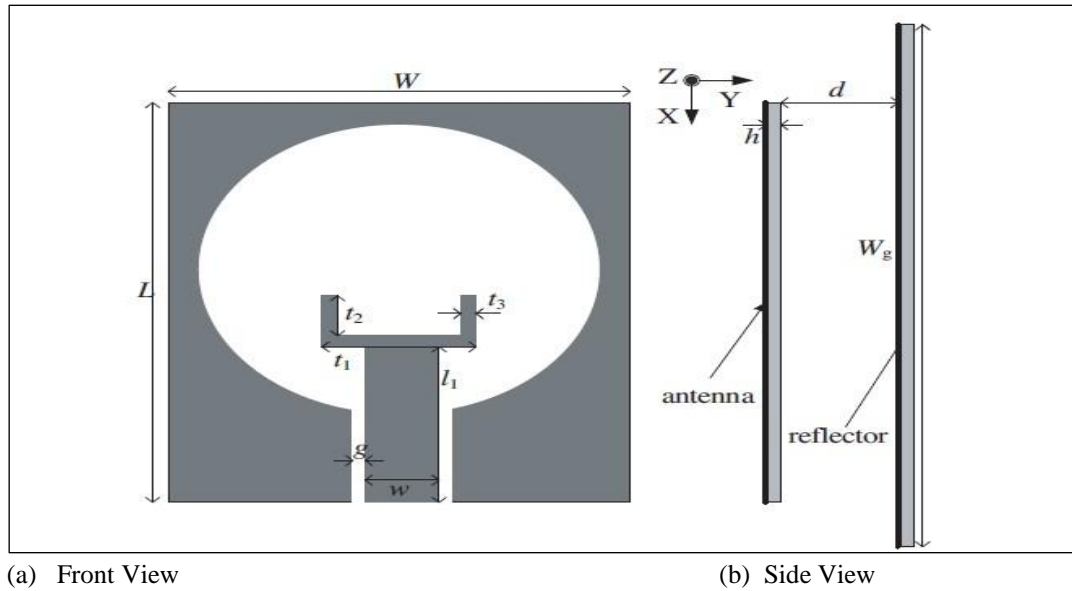


Figure 6: Configuration of Reference Directional UWB Antenna with Fork-shaped Stub (Reference antenna 2). Source: [6].

The above referenced antenna 2 was also examined by authors in [6], the antenna is a UWB Slot Antenna excited by fork-shaped tuning stub and it was later compared to the reference antenna 1 which is the Coplanar Waveguide fed UWB Slot Antenna. Here the circular radiator was removed and replaced with a fork-shaped tuning stub. The feed line is described by parameter l_1 while the other dimensions are kept constant as the CPW Fed UWB Slot Antenna. The main reason for replacing the circular patch with a fork-shaped tuning stub is to obtain a large impedance matching. The same size of reflector added to the CPW fed UWB

antenna was also added to this UWB Slot antenna so as to increase the directivity.

The reflection coefficient was also simulated in terms of the distance d between the antenna and the reflector and it was plotted on a graph against the frequency. The result gave a good performance of impedance matching at low frequency band although, the impedance matching was very poor at a high frequency band and it can be seen from the reflection coefficient graph in Figure 7 that the bandwidth of the antenna becomes narrower as the distance decreases [6-10].

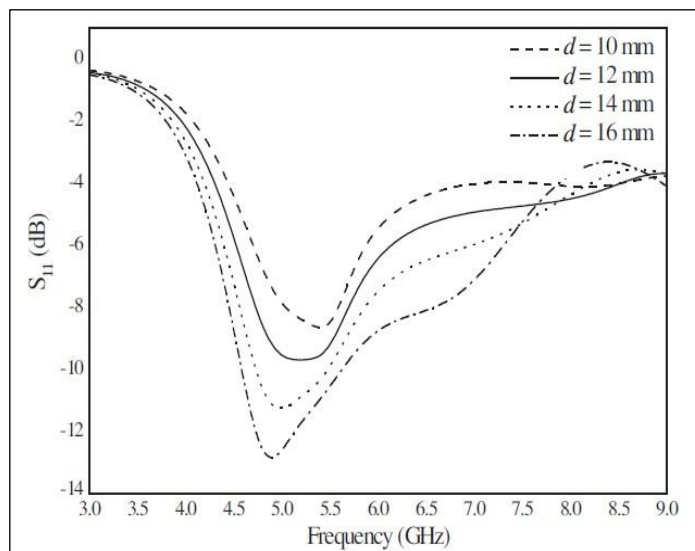


Figure 7: Simulated Return Losses in Terms of Distance d . Source: [6].

After proper examination, it can be deduced that both antennas discussed have their shortcomings. The shortcoming of both reference antenna 1 and reference antenna 2 is that reference

antenna 1 has a poor impedance matching at lower frequencies band while reference antenna 2 has a poor impedance matching at high frequencies band when the distance between the antenna and

the reflector is very small. A low profile antenna as shown in Figure 3 was designed by to eliminate the shortcomings of both reference antennas discussed earlier. The antenna was designed so as to cover both low and high frequencies band. This antenna was designed and compared to both reference antennas 1 and 2. When compared with Coplanar Waveguide fed UWB slot antenna, the slot ground and feed line are moved from top layer to bottom layer and the feed line has been changed to fork-shaped tuning stub. This antenna

designed by [6] can also be seen as a the composition of UWB slot antenna excited by fork-shaped tuning stub which is the reference antenna 2 on bottom layer and a circular patch on top layer respectively. It was ensured that the reflector's dimension is the same for the three types of UWB antenna and the dimension of the radiator is the same as the coplanar waveguide fed UWB slot antenna.

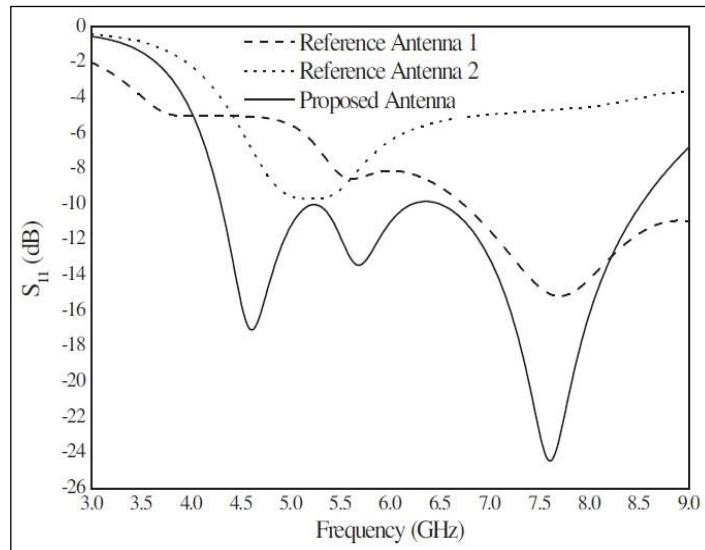


Figure 8: Simulated Reflection Coefficients among the three Types of Antenna.
Source: [6].

The simulated reflection coefficient among the three types of antennas as seen in Figure 8 shows that the proposed directional antenna has a better impedance matching at low frequency band when compared with the CPW fed UWB slot antenna (reference antenna 1) because of the separation of the slot ground plane on the bottom layer from the circular patch on the top layer and also seen to be improved at a high frequency band because of the circular patch added when compared with the Fork-shaped excited UWB slot antenna (reference antenna 2). In terms of the antenna gain, the proposed directional antenna has the same variation trend with the Fork-shaped excited UWB slot antenna over the whole frequency band. It has a higher gain than the fork-shaped excited UWB slot antenna because of the circular patch radiation. When compared with the CPW fed UWB slot antenna, the gain greatly improved from about 4GHz to 6GHz due to a good impedance matching.

The major challenge of the design of a compact coplanar waveguide-fed ultra-wideband monopole-like slot antenna earlier reviewed by [11] was the emission of energy as a result of back radiation which made it not completely unidirectional and this is the more reason why the author wouldn't be agreeing with this design and the author thought there should be possible ways of reducing the back radiation and a way to further improve the impedance matching of the antenna which made the author to further his research on how to achieve a unidirectional radiation over an Ultra-wideband frequency range and a way to improve the impedance bandwidth and reduce the back radiation.

Most of the UWB antennas presented so far exhibit radiation patterns similar to the acceptable monopole/dipole antennas. It is suspected that the antenna efficiencies will be degraded owing to omni-directional/bi-directional radiation when they are attached to the walls, metallic objects or the human body. To avoid the degradation on the antenna efficiencies, a directional UWB should be utilized which brought about the high desire for

the development of a UWB antenna having directional radiation characteristics [4] - [11].

III. MATERIALS AND METHODS

The research approach adopted was based on literatures with the highest level of methods and developments. A descriptive and quantitative approach is used. The major challenge in most antenna design is the emission of energy as a result of back radiation which makes the system not completely directional. Ways to avoid this emission of energy were discussed in the background study section of this paper which is the use of a reflector.

III.1 ANTENNA DESIGN

The prototype antenna was developed using a Computer Aided Design software- CST Microwave studio. A general purpose 3D Electromagnetic simulator known as the transient solver (Time domain) is used for the simulation. This solver gives results such as the S-parameters, modes of the port, far-field measurements of the designed antenna and many more. The parameter sweep option of the time domain is used to obtain multiple results which make the parametric study easier.

There are different types of UWB antennas ready for use in literature for different UWB applications. The choice of a UWB antenna depends on the particular application for which it will be used. For instance, omni-directional UWB antennas are used in mobile communications whereas directional UWB antennas are the most preferred antennas in UWB radar applications. The focus of this project is to design an antenna capable of operating over the entire UWB frequency range allocated by the FCC in 2002 with good directional radiation pattern. A small, simple and compact UWB antenna was simulated and fabricated.

III.2 ANTENNA STRUCTURE

The proposed antenna was implemented with a low cost FR4 substrate with a dielectric constant $\epsilon_r = 4.3$ and a thickness $h = 1.6\text{mm}$. Two models were simulated; the components of the first model are ground plane, substrate, inner patch and an inner feeder. The only difference between the first and the second model is the addition of another ground plane to serve as a reflector so as to increase the directivity of the antenna. The antenna is made up of

a rectangular aperture carved out from the ground plane of a printed circuit board (PCB) and a T-shaped stub for excitation. The antenna and the feeding structure are implemented on the same plane which makes the fabrication of the antenna cost effective and very easy. A micro-strip transmission line designed with characteristic impedance of 50Ω and a sub miniature connector was used for the termination during the measurement process. A compact aperture area of $13 \times 23\text{mm}^2$ is achieved. A quarter-wavelength is greater than the dimensions for the lowest UWB frequency (3.1GHz).

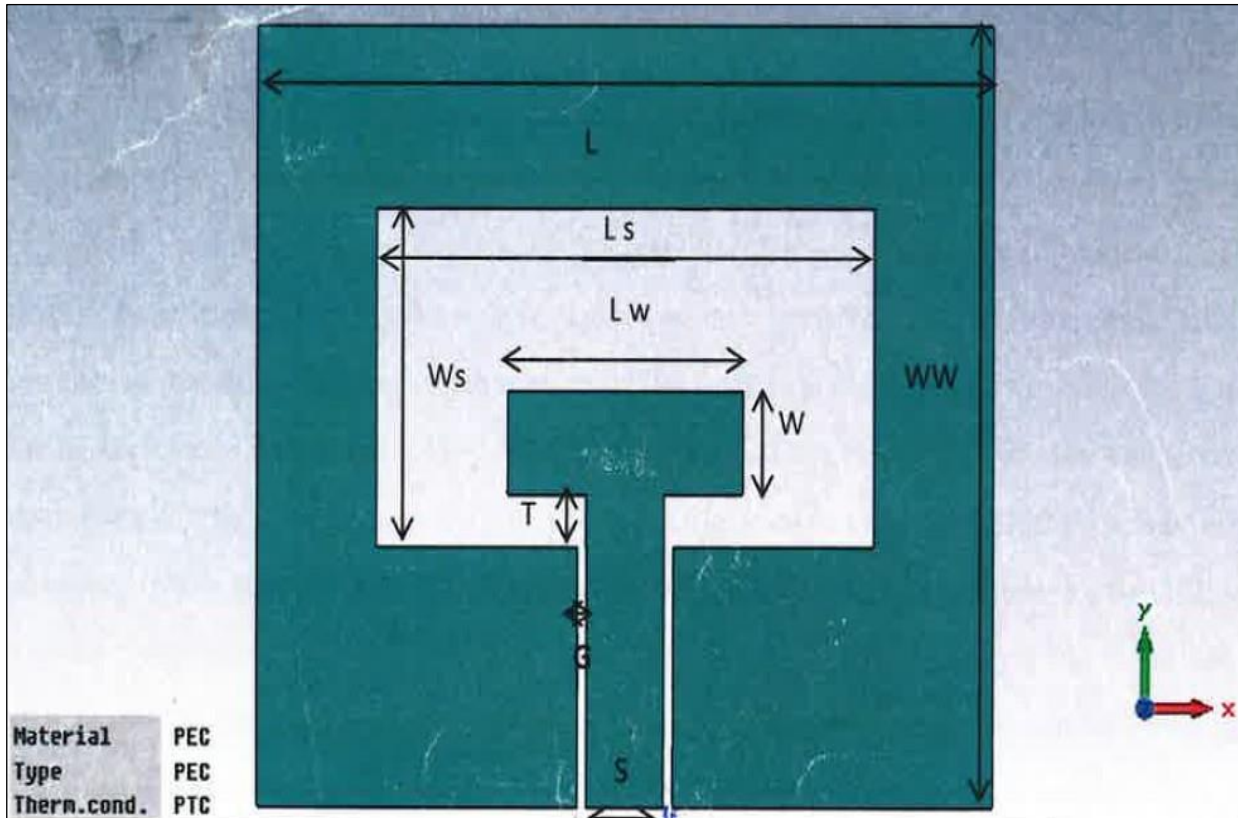


Figure 9: Geometry and Configuration of the Proposed Antenna.

Source: [10].

The geometry and configuration of the proposed antenna is shown in Figure 9. The length L_w , the width W , and the extrusion depth T are the only three parameters of the T-shaped stub [10]. The design parameters are $W_s = 13\text{mm}$, $L_s = 23\text{mm}$, $T = 2\text{mm}$,

$W = 4\text{mm}$, $L = 34\text{mm}$, $WW = 30\text{mm}$, $S = 3.6\text{mm}$, $G = 0.4\text{mm}$, $L_w = 10.8\text{mm}$, $S_1 = 12$, $t_{\text{patch}} = 0$ and $t_{\text{sub}} = 1.6\text{mm}$. The dimension of the components was calculated. Table 1 shows the dimensions used for the components.

Table 1: Table showing the Dimensions used for the Components.

Components	X_{\min}	X_{\max}	Y_{\min}	Y_{\max}	Z_{\min}	Z_{\max}
Inner patch	$-LW/2$	$LW/2$	T	$T+W$	0	t_{patch}
Inner feeder	$-S/2+G$	$S/2-G$	$-S_1$	T	0	t_{patch}
Substrate	$-L/2$	$L/2$	$-S_1$	$WW-S_1$	$-t_{\text{sub}}$	0
Ground	$X_p(1)$	$X_p(2)$	$Y_p(1)$	$Y_p(2)$	0	0

Source: Author, (2023).

A well designed model was obtained after using the above dimensions for the individual component. After that, a waveguide

port was added to it before simulation commenced. The dimension of the port is shown in Table 2.

Table 2: Table showing the Dimensions of the Waveguide Port,

Port	$X_{\min} = -S/2-G-t_{\text{sub}}*3$	$X_{\max} = S/2+G+t_{\text{sub}}*3$	$Z_{\min} = -1.6-5$	$Z_{\max} = 7$
------	--------------------------------------	-------------------------------------	---------------------	----------------

Source: Author, (2023).

Figure 10 shows the picture of the first model designed using CST microwave studio, ready for simulation.

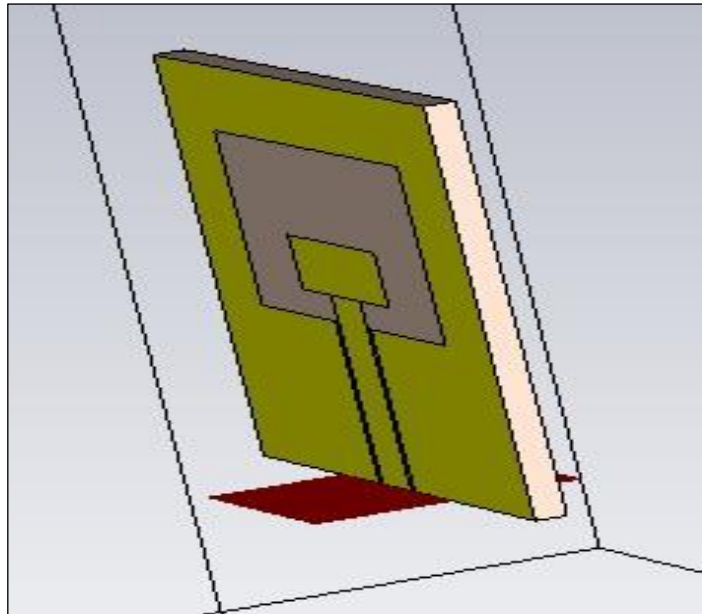


Figure 10: Designed Model of the Proposed Antenna with one Ground Plane.
Source: Author, (2023).

III.3 PARAMETRIC STUDY

The commercial simulation tool CST Microwave Studio is used in this research to perform the design and the optimisation

process. The effect of parameters L_w , W , T , W_s and L_s on the input impedance is carried out using the parameter sweep option of the time domain solver. Figures 11 – 15 shows the effects of variation of the five parameters respectively.

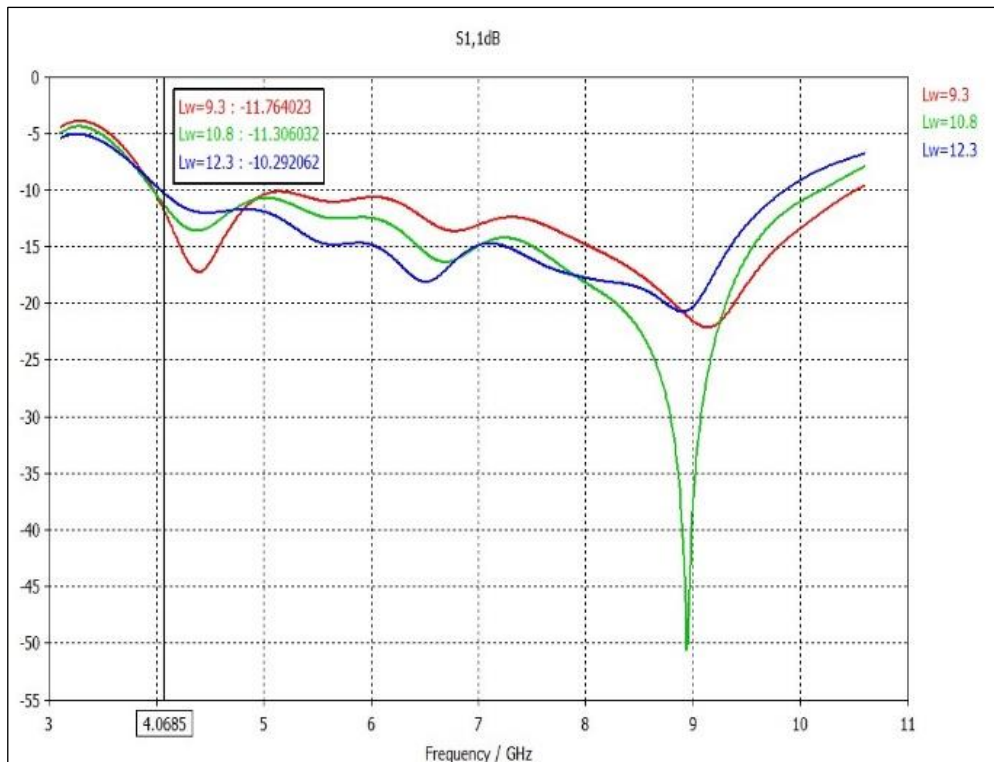


Figure 11: Effects of the Variation of Length L_w of the Antenna with one Ground Plane.
Source: Author, (2023).

The return loss of the proposed antenna with one ground plane when the length L_w was varied with comparison to the initial value of 10.8mm is shown in Figure 11. It can be seen from the S11 graph that the return loss at low frequencies 3.1-4.06GHz is higher

than -10dB which implies a poor performance at that frequencies band but there is a decrease in the return loss at frequencies 4.06-5GHz, a greater decrease is observed at these frequencies band when the length is decreased to 9.3mm, but at higher frequencies

of 8.6-9GHz, the return loss decreases even more at the initial length of 10.8mm. Increase in return loss simply means that reflected power also increases while a decrease of the return loss

means there is a better improvement of the system because of the low power reflected back due to impedance mismatch.

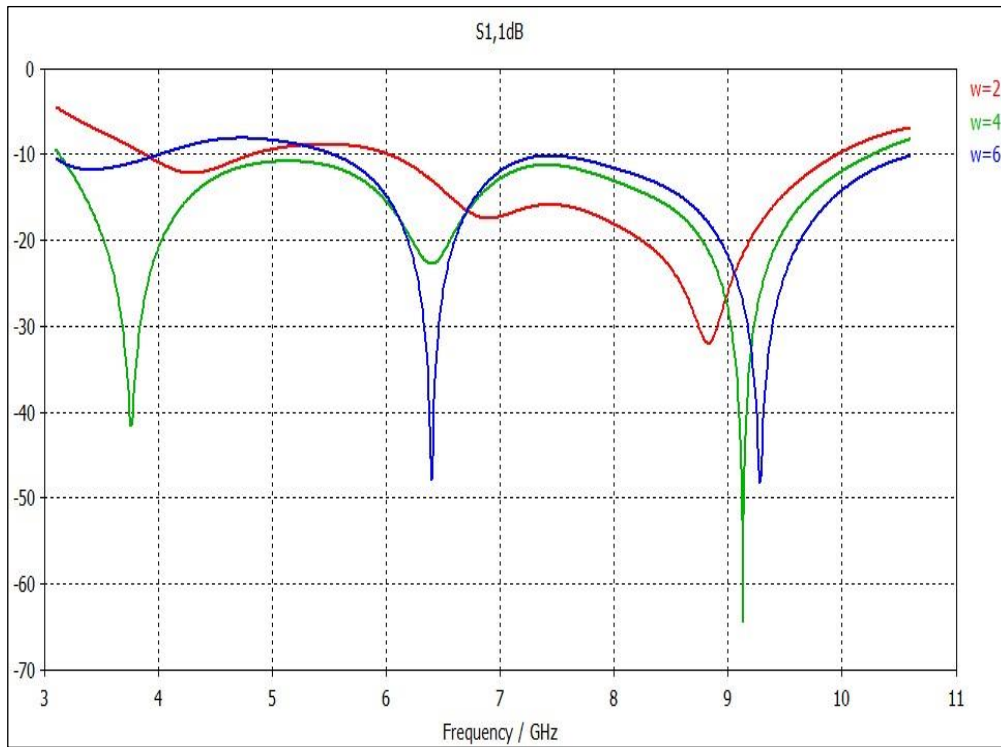


Figure 12: Effects of the Variation of Width W of the Antenna with one Ground Plane.
Source: Author, (2023).

The dimensions of other parameters still remain the same as $L_w=10.8\text{mm}$, $L=34\text{mm}$, $L_s=23\text{mm}$, $WW=30\text{mm}$, $S=3.6\text{mm}$, $G=0.4\text{mm}$, $W=4$, $W_s=13\text{mm}$ and $T=2\text{mm}$. Figure 12 represents the return loss of the designed antenna with one ground plane when the width of the T-shaped was varied. The return loss increases at

frequencies band of 3.1-6.4GHz and 9.2-10.6GHz when the width W was reduced by 2 compared to the initial width $W=4$, but it decreases between 8-9.2GHz. This increase means that the antenna transmits less power.

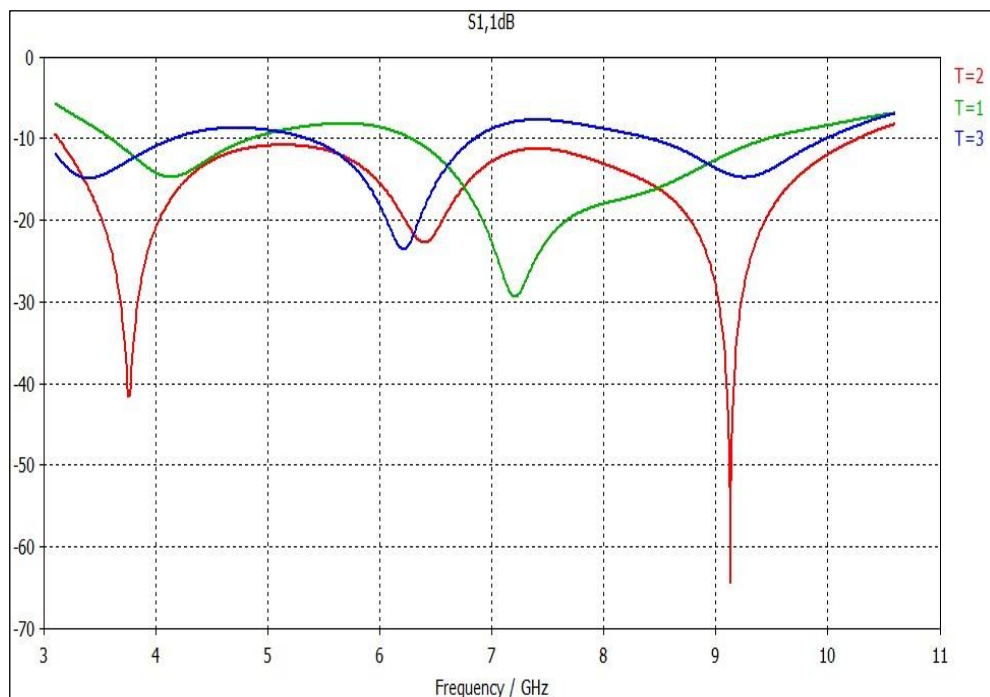


Figure 13: Effects of the variation of extrusion depth T of the antenna with one ground plane.
Source: Author, (2023).

Figure 13 shows the variation of the return loss when the extrusion depth T of the T-shaped of the proposed antenna with one ground plane was varied. This variation of T aggravated a big increase in the return loss between frequencies of 3.2GHz to about

6.5GHz and 7.3GHz to 10.6GHz but it decreases between 6.5GHz to 7.3GHz when T is reduced to 1mm. When T decreases, less power is being transmitted by the designed antenna.

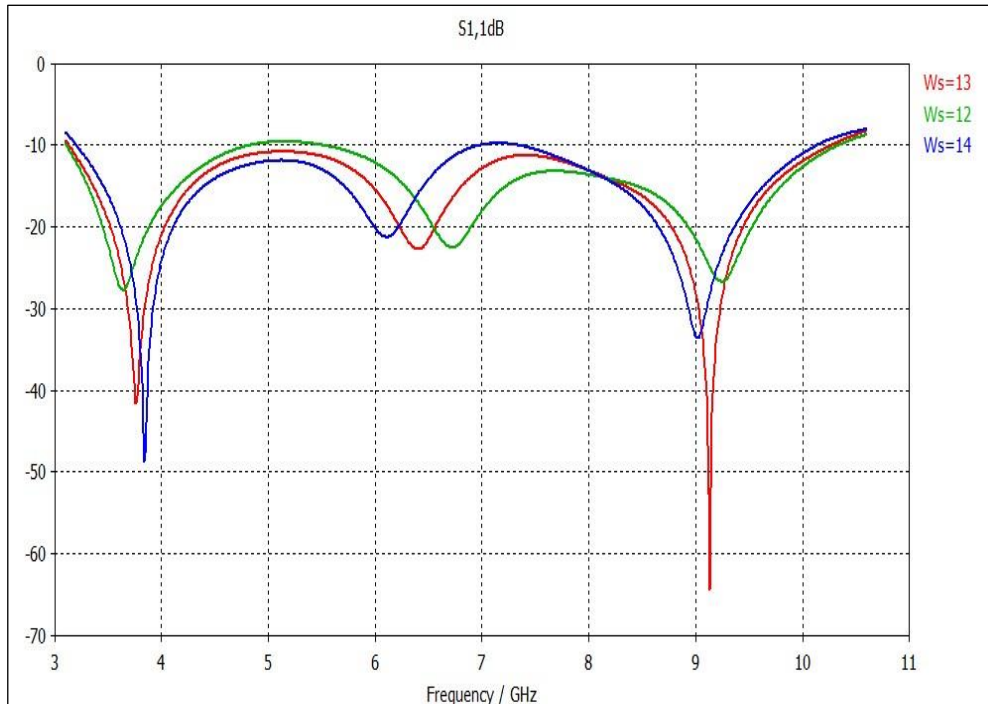


Figure 14: Effects of Variation of Width W_s of the Antenna with one Ground Plane.
Source: Author, (2023).

The dimension of other parameters were kept constant during this optimisation process. As seen in Figure 14, the return loss of the designed antenna when the length W_s was varied with comparison with the initial value of $W_s=13$ mm seems better compared to other parameters varied earlier as $S_{11} \leq -10$ dB is maintained almost throughout the operating frequencies band. As the length W_s was reduced to 12mm, the return loss increases at

3.6GHz to 6.5GHz and at 8.2GHz to 9.2GHz but it decreases at starting frequency of 3.1GHz to 3.5GHz, middle frequencies of 6.5GHz to 8GHz and higher frequencies 9.3GHz to 10.6GHz. The decrease in the return loss means that the antenna is radiating a high percentage of its power between those frequencies band while the increase in the return loss brings about a good performance of the system as the antenna radiates less power at those frequencies band.

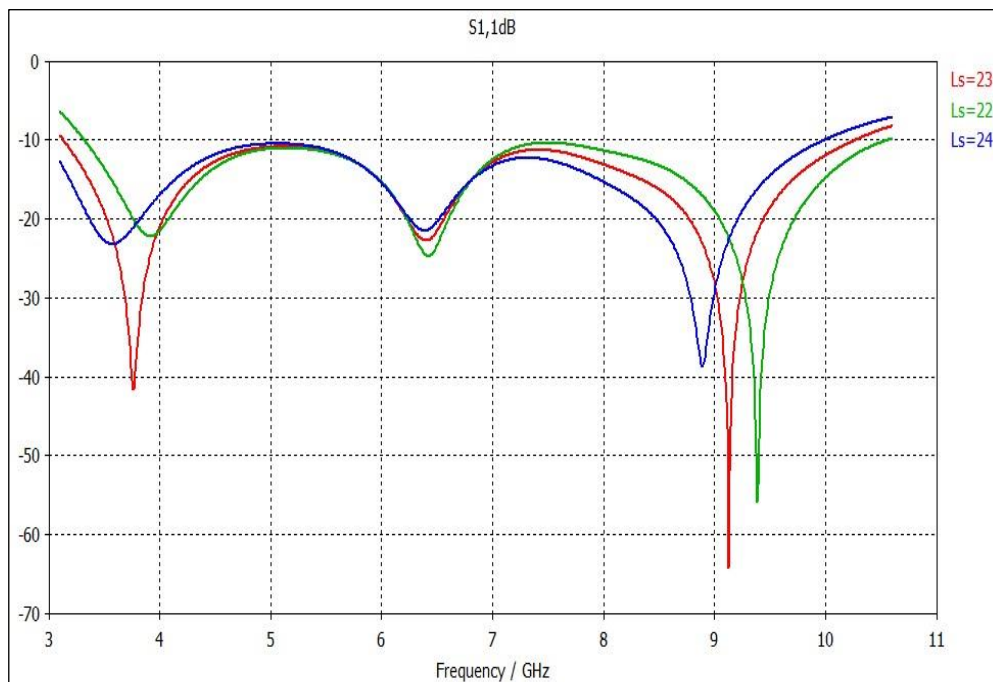


Figure 15: Effects of the Variation of Length L_s of the Antenna with one Ground.
Source: Author, (2023).

Figure 15 illustrates the effects of the variation of the aperture length of the antenna on the return loss of the system. The reduction of L_s to 22mm influences the middle frequencies band. At these frequencies band, the antenna radiates more power than the initial parameter of $L_s=23$ mm. Increase of L_s to 24mm provokes an increase in the return loss at 3.6GHz to 6.2GHz.

III.4 RADIATION CHARACTERISTICS

An omni-directional radiation pattern is obtained from the simulation of the designed model with one ground (first model) as

it radiates forward and backward when implemented at frequencies of 5GHz, 8GHz and 10GHz. Figures 16 – 18 shows the 3D plots of the radiation pattern of the first model of the proposed antenna at 5GHz, 8GHz and 10GHz respectively. It can be seen that there's more gain in the x-direction than the other directions and for all the three different frequencies, energy is more radiated at x-direction than in the y and z directions. Two notches can be seen along the Y axis where there is no radiation at all. At frequency of 5GHz, the realised gain is 3.31dB which can be seen in the x-plane in Figure 16, while a gain of 0.414dB and -22.9dB was achieved at y-plane and z-plane respectively.

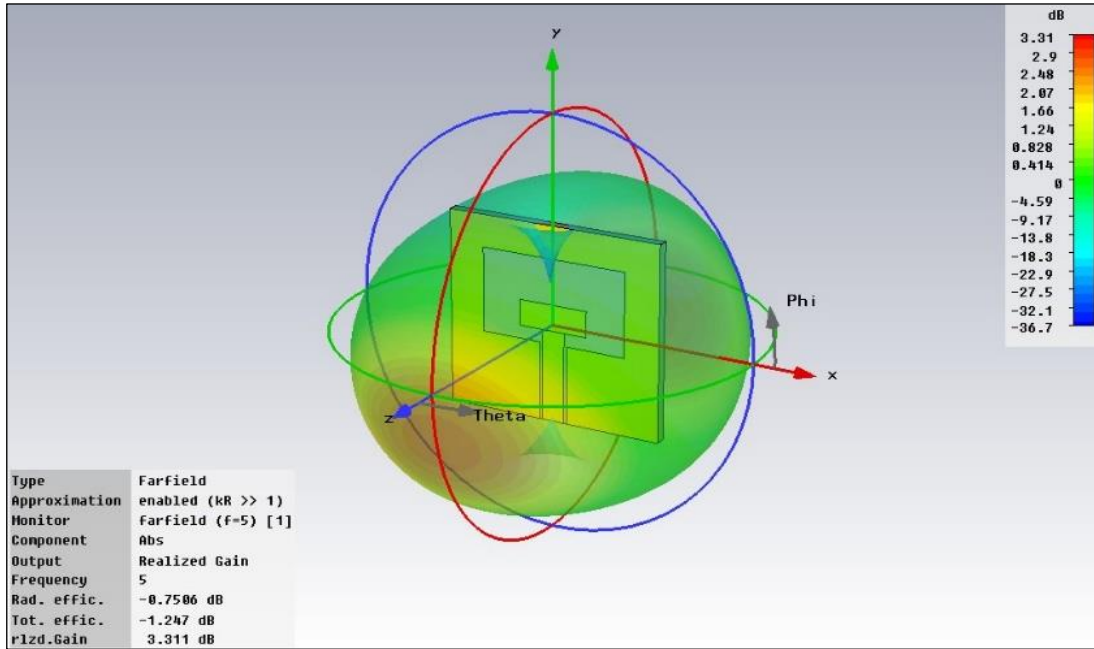


Figure 16: Radiation Pattern at 5GHz in 3D Plot.
Source: Author, (2023).

At the two other frequencies, that is, 8GHz and 10GHz, it can be seen that a realized gain of 3.362dB and 3.302dB was achieved as shown in Figures 17 and 18.

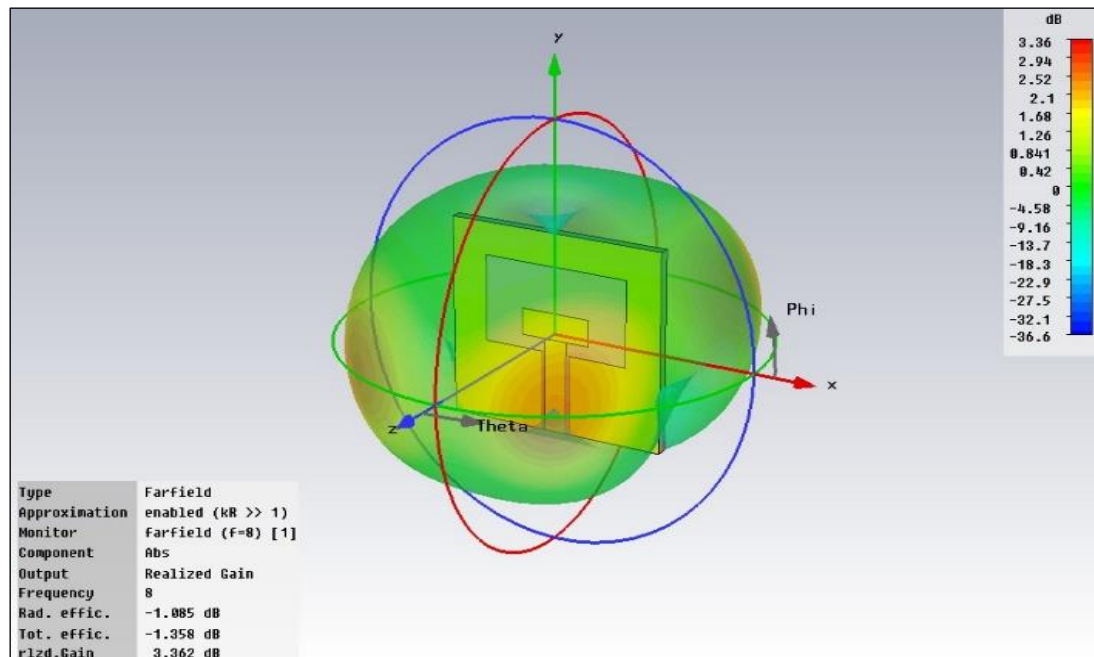


Figure 17: Radiation Pattern at 8GHz in 3D Plot.
Source: Author, (2023).

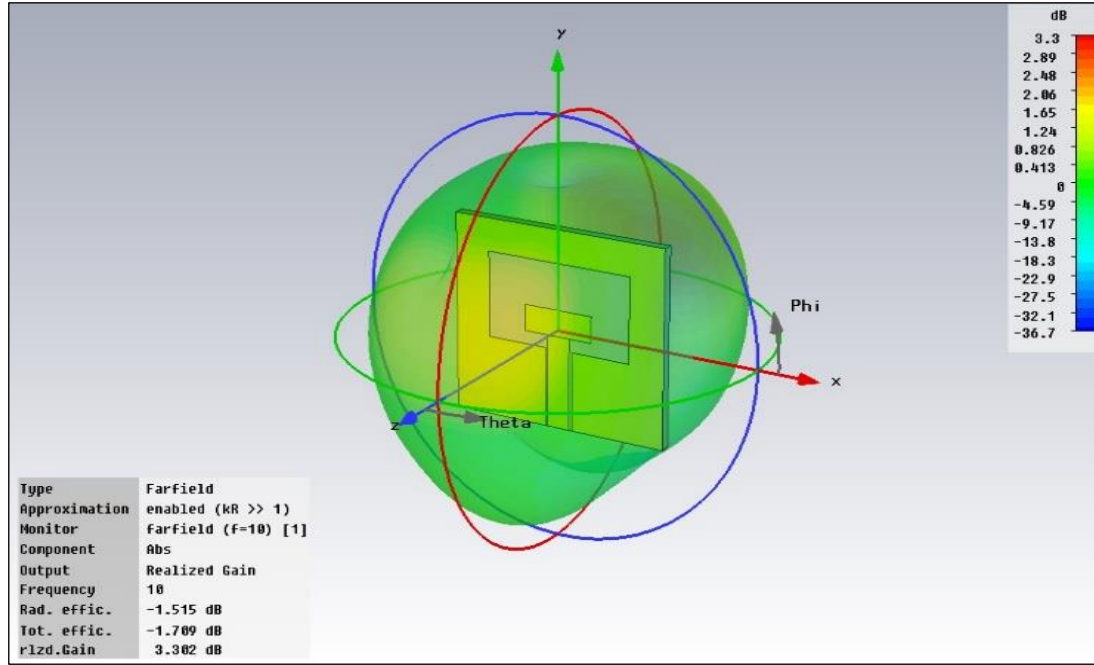


Figure 18: Radiation Pattern at 10GHz in 3D Plot.
Source: Author, (2023).

The first model was designed and simulated using the CST microwave studio; a parametric study was carried out so as to discover the effect of the parameters on the input impedance of the system likewise the radiation pattern. It can be seen that the antenna exhibits an omni-directional radiation pattern. A further experiment to achieve the aim of this research was further carried out by the author, which is to obtain a directional radiation pattern.

III.5 INVESTIGATIONS ON INPUT IMPEDANCE AND RADIATION PATTERN USING THE SECOND MODEL

Investigation was done using the second model which comprise of substrate, an inner feeder, inner patch, ground plane and an additional ground plane was added to it which serves as a reflector. The dimensions of the inner feeder, inner patch, substrate and the ground plane were kept constant as in the previous model while the dimension of the reflector was added. Table 3 shows the dimensions of the reflector where LF= 60mm, Lf_offset= 25mm and Wf= 60mm.

Table 3: Table showing the Dimensions of the Reflector.

Component	Umax	Vmin	Vmax	Wmin	Wmax
Reflector	Wf/2	-Lf_offset	-Lf_offset+LF	-df	df

Source: Author, (2023).

The starting point for this investigation after reviewing different literatures was to calculate the distance at which the reflector would be positioned to the substrate. This reflector was placed at a distance of a quarter-wavelength to the substrate. The value of the quarter wavelength was calculated using the formula:

$$\lambda = c/f \tag{1}$$

Where $c = 3 \times 10^8$ m/s and f is the centre of the frequency band. Therefore,

$$f = \frac{3.1 + 10.6}{2} = 6.85 \text{GHz}$$

$$\lambda = 3 \times 10^8 \div 6.85 \times 10^9 = 0.0437 \text{m}$$

$$\text{Quarter wavelength} = \frac{\lambda}{4} = \frac{0.0437}{4} = 0.0109 \text{m}$$

$$0.0109 \text{m} = 10.9 \text{mm}$$

This value is an estimated value of the quarter-wavelength at which the reflector was placed to the substrate as the effect of the substrate ($\epsilon_r = 4.3$) is ignored. Figure 19 shows the picture of the model with the reflector ready for simulation.

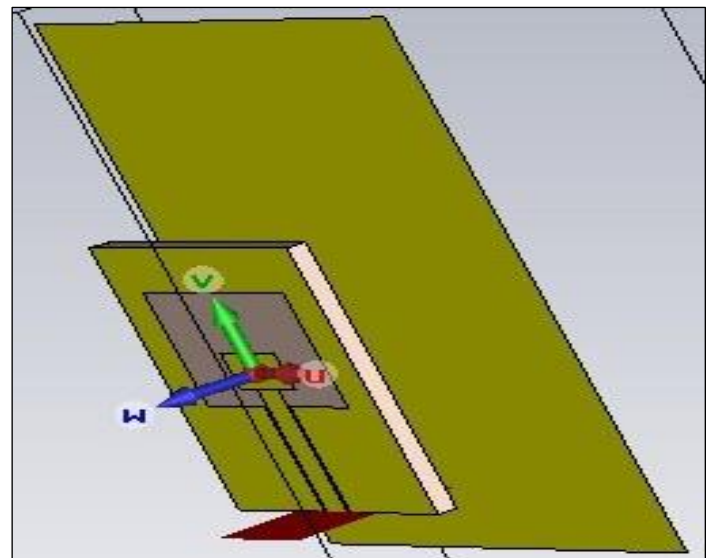


Figure 19: Picture of the Designed Model of the Proposed Antenna with a Reflector.
Source: Author, (2023).

The designed proposed antenna with reflector is now ready for the optimisation process. The effect of parameters L_w and W_s on the input impedance were carried out using the parameter sweep

option of the time domain solver just as it was done in the case of the first model. Figures 20 – 21 shows the effects of the variation of the parameters.

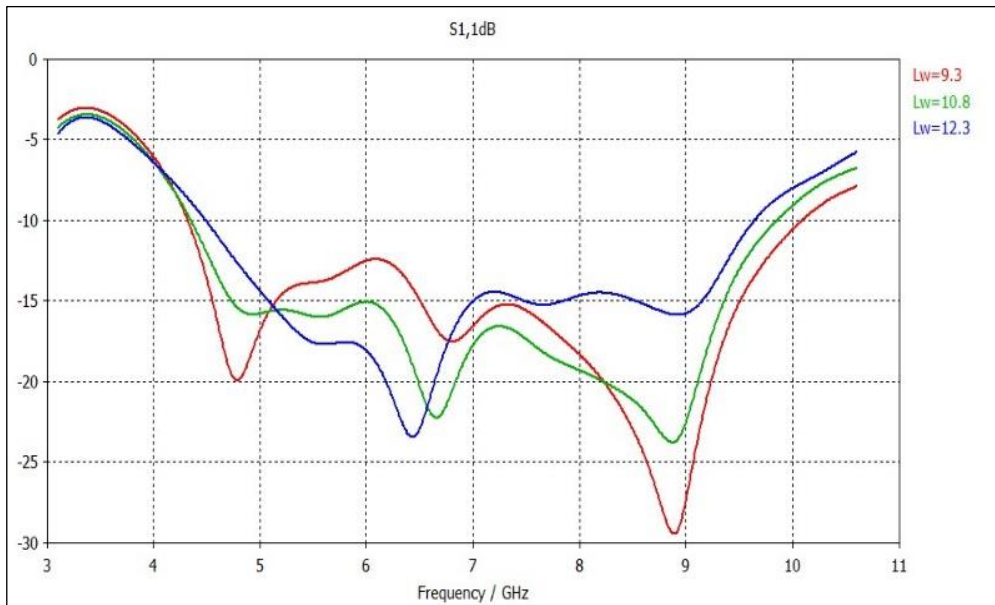


Figure 20: Effects of the Variation of Length L_w on the Model with Reflector.
Source: Author, (2023).

The dimension of other parameters are $L=34\text{mm}$, $W_s=13\text{mm}$, $W=4\text{mm}$, $L_s=23\text{mm}$, $WW=30\text{mm}$, $S=3.6\text{mm}$, $G=0.4\text{mm}$ and $T=2\text{mm}$. As illustrated in Figure 20, it can be seen that the return loss at frequencies 5GHz to 6.5GHz decreases when the length L_w was increased to 12.3mm when compared with the initial length of 10.8mm and it increases at frequencies 6.5GHz to 10.6GHz. This increase of the return loss for the frequencies band 6.5GHz to 10.6GHz means that the reflected power increases while the decrease of the return loss at frequencies band 5GHz to 6.5GHz

implies that there is a good improvement of the system because of the low power reflected back due to impedance mismatch. The antenna transmits less power between the frequencies band 6.5GHz to 10.6GHz. However, when L_w is reduced to 9.3mm, the return loss increases between 5.1GHz to 8.2GHz but decreases at lower frequencies band 4.3GHz to 5GHz and higher frequencies band 8.3GHz to 10.6GHz. Less power is reflected back at these frequencies, which bring about a good performance of the system.

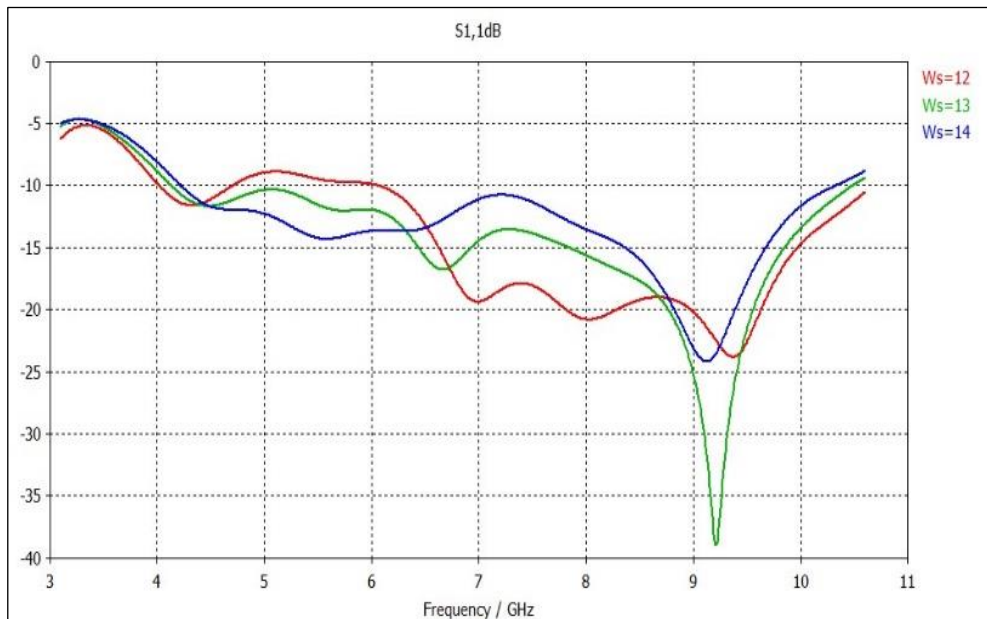


Figure 21: Effects of the Variation of Width W_s on the Model with the Reflector.
Source: Author, (2023).

When the width W_s was varied with comparison with the initial value of 13mm, it can be seen from the return loss plot in Figure 21 that there is an increase in the return loss at frequencies

of 4.5GHz to 6.6GHz when the width was reduced to 12mm but it decreases at 6.7GHz to 8.7GHz. The decrease of the return loss means that the proposed antenna radiates a larger percentage of its

power between frequencies band 6.7GHz to 8.7GHz while less power is being transmitted but in the case of when the value of W_s was increased to 14mm, the return loss increases between the frequencies band 6.5GHz to 8.8GHz and 9.2GHz to 10.6GHz. The system is said to be improved when the return loss increases and the antenna radiates less power.

An overall better performance of the system is obtained as seen from the results obtained from the investigations on the second model (proposed antenna with a reflector) as carried out in the experiment. The reflection coefficients (S_{11}) as a function of frequency for the proposed antenna with a reflector are illustrated in Figures 20 and 21. The antenna demonstrates good impedance bandwidth ($S_{11} \leq -10\text{dB}$) from about 4GHz to 10.6GHz except in the case of when the width W of the T-shaped stub was varied. The radiation patterns of the two models were analysed and compared. A good directivity was achieved by the proposed antenna with a reflector compared to the one without a reflector.

IV. RESULTS AND DISCUSSIONS

The return loss of the proposed antenna is obtained using the network analyser. Proper calibration of the network analyser is necessary before measurement commences since the length of the feed-line changes significantly electrically as it sweeps the frequency from low to high. This calibration also helps in the elimination of all forms of errors such as errors from the cable and ports. The calibration was done using the calibration kits comprising the calibration tools such as Broadband load, Short load 053537 and Open load 053669. The frequency of interest was required for the measurement; the frequency band for the proposed antenna which is 3.1-10.6GHz was set by inputting 3.1GHz as the start frequency and 10.6GHz as the stop frequency. These three calibration tools named earlier are all 3.5mm she-male connector

which was used to calibrate the device. The broadband load was the first tool used in calibrating the network analyser, followed by short load and then open load. The port 4 of the network analyser was used for the measurement; these tools were connected one after the other to the he-male connector of the port 4 of the network analyser to carry out the calibration. The Antenna under test was measured immediately the calibration sequence was completed.

A sharp curve at lower frequencies of 4.2-5.8GHz and higher frequencies of 8-10GHz can be seen from the return loss of the measured and simulated results respectively in Figure 22 This curve shows a decrease in the return loss which implies that the proposed antenna transmit higher percentage of its power at these frequencies while a very low power is reflected back. An increase in return loss is observed at frequencies of 5.8-6.4GHz from the measured result, at this point, the antenna transmits less power.

The simulated and the measured results do not completely agree with each other as it can be seen in Figure 22 showing the comparison between them. The system impedance bandwidth dropped from 6.6GHz to 5.8GHz from 4.2-10GHz with a return loss greater than 10dB, except in the band of 5.8-6.4GHz and 10-10.6GHz. This difference between the simulated and measured results might be caused by the fabrication and measurement inaccuracies of the prototype. Another reason for such disagreement could be being that the measurement was carried out in a non-controlled environment. A lump port of 50Ω considered being loss-less is fed to the simulated antenna which is hard to achieve in fabrication especially for low cost materials. Losses due to soldering of the SMA connector and also the microwave cable used for measurements could be another cause for this disagreement. Finally, another possible reason for such disagreement between the simulated and measured results could be as a result of cable currents which often have effects on the measurement results.

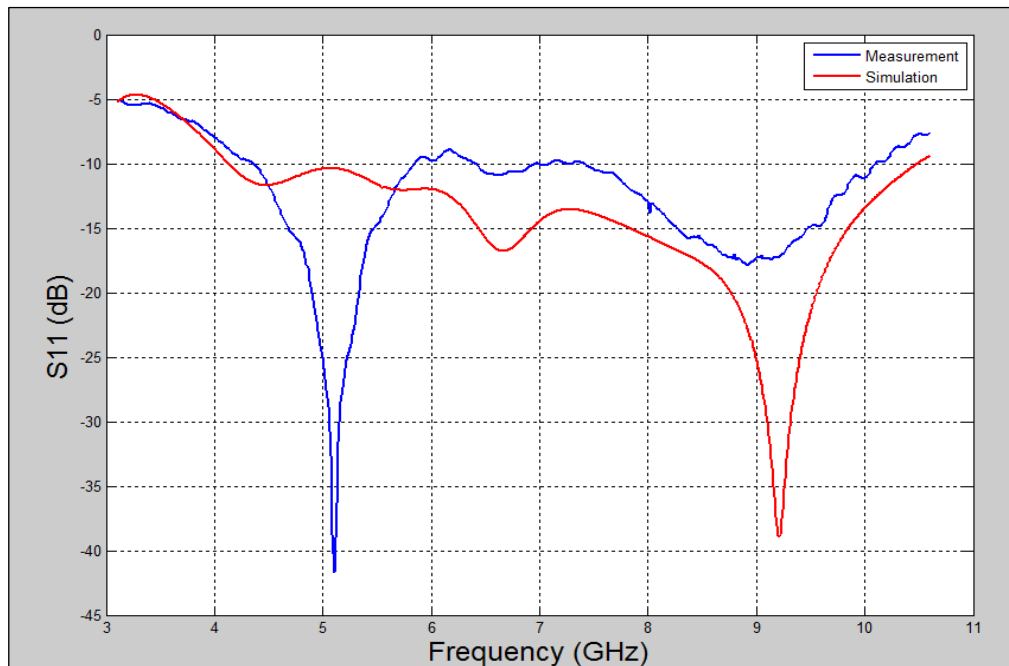


Figure 22: Return Loss of the simulated result with Comparison with the Measured Result.
Source: Author, (2023).

Figure 23 shows the measurement set up of the proposed antenna with reflector in the far-field anechoic chamber. The Antenna under test (AUT) which is the receiving antenna is separated by enough distance from the transmitting antenna so as

to excite the designed operating environment. This distance separation is determined using this mathematical formula below;

$$R > \frac{2D^2}{\lambda} \quad (2)$$

Where R is the separation distance between the transmitting and receiving antennas, D is the aperture of the antenna under test (AUT) and λ is the measurement wavelength. The frequencies at which the radiation pattern of the proposed antenna was implemented are 3GHz, 4GHz, 5GHz and 6GHz. At

360° theta, the far-field is better at 5GHz and best at 6GHz giving a good directional radiation pattern. At frequencies of 3GHz and 4GHz, the opposite is the case giving an omni-directional radiation pattern. The radiation pattern of the proposed antenna with reflector as measured in the far-field anechoic chamber is shown in Figure 24.

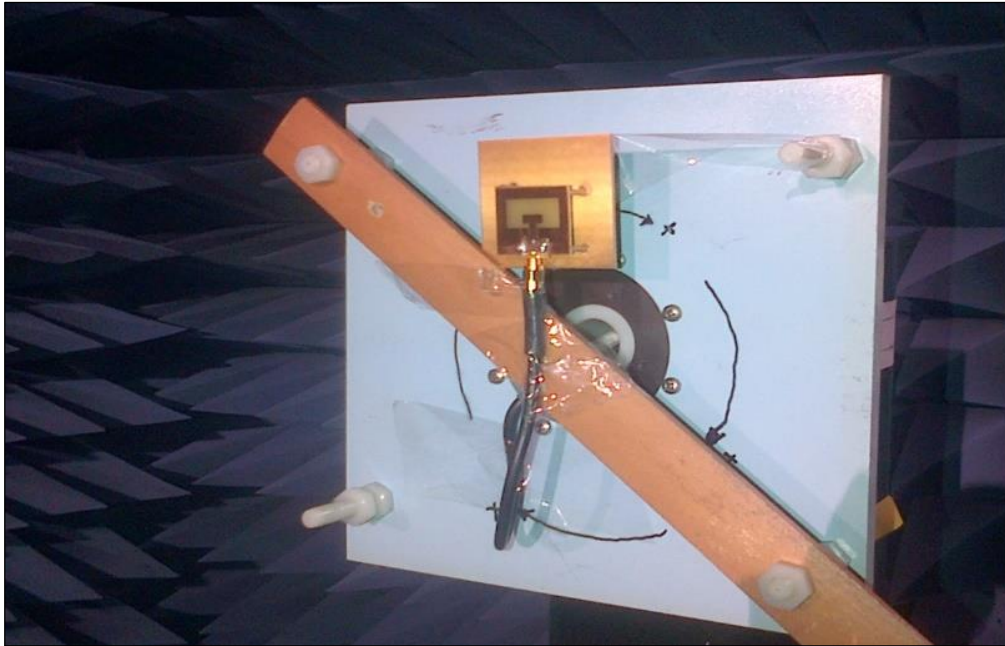


Figure 23: Measurement set-up of the Proposed Antenna with Reflector in the Anechoic Chamber. Source: Author, (2023).

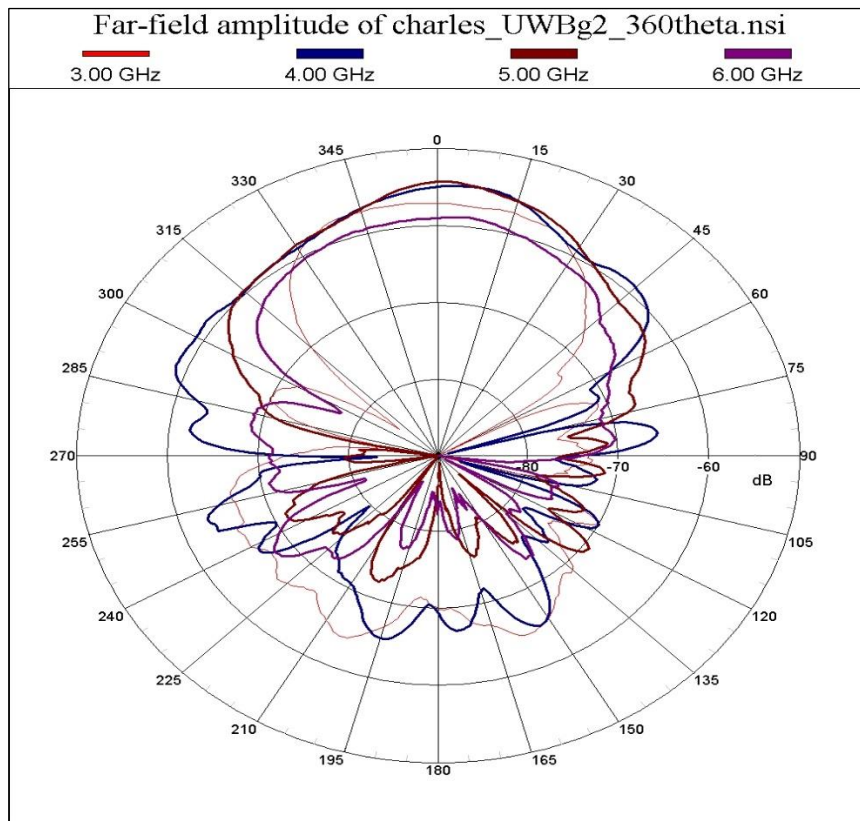


Figure 24: The Measured far-field Amplitude Radiation Pattern of the Proposed Antenna. Source: Author, (2023).

The measured radiation patterns broadly agree with the simulated radiation patterns. An omni-directional radiation pattern

is achieved at 3GHz and 4GHz while a directional radiation pattern is achieved at frequencies of 5GHz and 6GHz. The measured

radiation patterns are normalised patterns while the simulated radiation patterns are not normalised. Investigations were carried out to see if a better radiation pattern could be achieved at the frequencies of 3GHz and 4GHz.

The proposed antenna is printed on a FR4 printed circuit board. A 60x60mm² reflector was printed as well. The proposed antenna and the feeding structure are formed on the same side of the printed circuit board which makes the design easy and extremely low cost. The antenna was placed at a quarter-

wavelength distance to the reflector. It is fed by a 50Ω micro-strip line and a SubMiniature version A (SMA) connector is used for the port which was carefully soldered to the antenna in the communication lab. The photograph of the antenna with a reflector is illustrated in Figure 25. The return loss of the antenna is measured using the network analyser while the far-field amplitude radiation pattern is measured in the anechoic chamber of the communication lab.

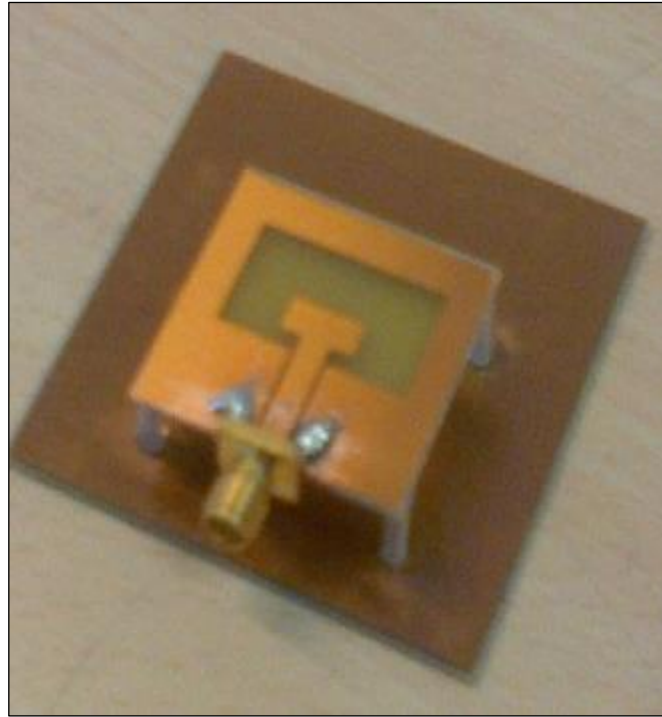


Figure 25: Photograph of the Proposed Antenna placed at a Quarter-wavelength Distance to the Reflector.
Source: Author, (2023).

V. CONCLUSIONS

In this study, a directional UWB antenna has been presented. Several types of UWB antennas have been analysed and the results compared. First and foremost, the background of the technology, applications and several techniques were discussed. Ways to avoid the major challenge in most antenna designs which is the emission of energy as a result of back radiation which makes the system not completely directional have been discussed. A commercial simulation tool known as CST Microwave Studio was used to carry out the design and the optimisation process. Two models were designed; the first model exhibits an omni-directional radiation pattern while the second model exhibits a directional radiation pattern except at frequencies of 3GHz and 4GHz. The directional radiation pattern is achieved as a result of the addition of another ground plane which serves as a reflector to the antenna. The antenna prototype is printed on a FR4 PCB with a specified overall dimension. The network analyser was used to measure the return loss of the fabricated antenna and the radiation pattern of the antenna was measured in the far-field anechoic chamber of the communication lab at 3GHz, 4GHz, 5GHz and 6GHz. Investigations were further carried out on how the directivity of the designed antenna can be improved at frequencies of 3GHz and 4GHz. This investigation was done by examining the effect of the size of the additional ground plane known as the reflector on the radiation pattern of the antenna using the simulation tool- CST Microwave Studio. Directional radiation patterns, except at 3GHz

and 4GHz, impedance bandwidth of 4.2-10GHz with a return loss greater than 10dB, except in the band of 5.8-6.4GHz and 10-10.6GHz are realised. The measured and simulated results have also been compared. The simulation and measurement results of the proposed antenna show a good agreement in terms of the radiation patterns but do not completely agree in terms of return loss as an unexpected behaviour was exhibited by the Antenna under test (AUT) as seen from the measured result in Figure 22 which could be as a result of cable current.

VI. AUTHOR'S CONTRIBUTION

Conceptualization: Olayiwola Charles Adesoba.

Methodology: Olayiwola Charles Adesoba.

Investigation: Olayiwola Charles Adesoba.

Discussion of results: Olayiwola Charles Adesoba.

Writing – Original Draft: Olayiwola Charles Adesoba.

Writing – Review and Editing: Olayiwola Charles Adesoba.

Resources: Olayiwola Charles Adesoba.

Supervision: Olayiwola Charles Adesoba.

Approval of the final text: Olayiwola Charles Adesoba.

VII. ACKNOWLEDGMENTS

The author wishes to thank Dr. Yi Wang for his support and guidance during the practical aspect of the research and also for allowing me to make use of the laboratories, without him, this

research wouldn't have been achievable. I would also like to appreciate my family for their love, support and words of encouragement each time I am on a research work.

VIII. REFERENCES

- [1] R. G. Blanks *et al.*, "Effect of NHS breast screening programme on mortality from breast cancer in England and Wales, 1990-1998: Comparison of observed with predicted mortality", *British Medical Journal*, 321(7262), pp. 665 - 669, 2000, doi: 10.1136/bmj.321.7262.665
- [2] Canadian Breast Cancer Foundation, "Earlier Detection and Diagnosis of Breast Cancer: Recommendations and Scientific Review", [Online] Available at: www.cbcbf.org/central/AboutBreastHealth/EarlyDetection/Mammography/Pages/Benefits-and-limitations.aspx [Accessed 3 October 2022].
- [3] Federal Communications Commission (FCC), "First Report and Order" 02 - 48, 2002 s.l.: s.n.
- [4] X. Qing & Z. N. Chen, "Compact Coplanar Waveguide fed Ultra-wideband Monopole-like Slot Antenna", *IET Microwaves, Antennas and Propagation*, 3(5), pp. 889 - 898, 2009, doi: 10.1049/iet-map.2008.0075.
- [5] J. Y. Sze & K. L. Wong, "Bandwidth Enhancement of a Microstrip line-feed printed wide-slot Antenna", *IEEE Trans. Antennas and Propagation*, 49(7), pp. 1020 - 1024, 2001, doi: 10.1109/8.933480.
- [6] F. Zhu *et al.*, "Low Profile Directional Ultra-wideband Antenna for See-Through-Wall Imaging Applications", *Progress in Electromagnetics Research*, Volume 121, pp. 124 - 129, 2011, doi: 10.2528/PIER11080907
- [7] A. Elsherbini & K. Sarabandi, "Directive Coupled Sectorial Loops Antenna for Ultra-wideband Applications", *IEEE Antennas Wireless Propagation Letters*, Volume 8, pp. 576 - 579, 2009, doi: 10.1109/LAWP.2009.2020444.
- [8] B. Allen *et al.*, "Ultra-wideband Antenna and Propagation for Communications, Radar and Imaging", In: New Jersey: Wiley Press, pp. 134 - 135, 2007, doi: 10.1002/0470056843.
- [9] A. M. Abbosh *et al.*, "A Planar UWB Antenna with Signal Rejection Capability in the 4-6GHz band", *IEEE Microwave and Wireless Components Letter*, 16(5), pp. 278 - 280, 2006, doi: 10.1109/LMWC.2006.873500.
- [10] Y. Lin & K. Hung, "Compact Ultra wideband Rectangular Aperture and Band-Notched Designs", *IEEE Transactions on Antennas and Propagation*, 54(11), pp. 3075 - 3077, 2006, doi: 10.1109/TAP.2006.883982.
- [11] X. Qing & Z. N. Chen, "A Miniaturized Directional UWB Antenna", *IEEE International Symposium on Antennas and Propagation*, pp. 1470 - 1473, 2011, doi: 10.1109/APS.2011.5996572.
- [12] S. C. Hagness, A. Taflove & J. E. Bridges, "Three-Dimensional FDTD Analysis of a Pulsed Microwave Confocal System for Breast Cancer Detection: Design of an Antenna-Array Element", *IEEE Transactions on Antennas and Propagation*, 47(5), pp. 783 - 791, 1999, doi: 10.1109/8.774131.
- [13] I. Y. Immoreev, "Practical Applications of UWB Technology", *IEEE Aerospace and Electronic Systems Magazine*, 25(2), pp.36-42, 2010, doi: 10.1109/MAES.2010.5442175.
- [14] H. M. Jafari *et al.*, "Ultra-wideband Radar Imaging System for Bio-medical Applications", *Journal of Vacuum Science and Technology*, 24(3), pp. 752 - 757, 2006, doi: 10.1116/1.2194028.
- [15] J. Liang, "Antenna Study and Design for Ultra-wideband Communication Applications", "PHD Thesis, 9-10", 2006, London: Department of Electronic Engineering, Queen Mary University.
- [16] P. Li, J. Liang & X. Chen, "Study of Printed Elliptical/Circular slot Antennas for Ultra-wideband Applications", *IEEE Transaction on Antennas Propagation*, 54(6), pp. 1670- 1675, 2006, doi: 10.1109/TAP.2006.875499.
- [17] Z. N. Chen *et al.*, "Planar Antennas", *IEEE Microwave Magazine*, 7(6), pp. 63 - 73, 2006, doi: 10.1109/MW-M.2006.250315.
- [18] X. Qing, Z. N. Chen & M. Y. W. Chia, "UWB Characteristics of Disc-cone Antenna", *IEEE Proceedings on International Workshop of Antenna Technology*, pp. 97 - 100, 2005, doi: 10.1109/IWAT.2005.1461013.
- [19] Y. Ranga *et al.*, "Increasing the Gain of a Semicircular Slot UWB Antenna Using an FSS Reflector", *IEEE conference on Antennas and Propagation in Wireless Communications*, pp. 478-481, 2012, doi: 10.1109/APWC.2012.6324954.
- [20] A. J. Surowiec, S. S. Stuchly, J. R. Barr & A. Swarup, "Dielectric Properties of Breast Carcinoma and Surrounding Tissues", *IEEE Transaction Biomedical Engineering*, 35(4), pp. 257 - 263, 1988, doi: 10.1109/10.1374.
- [21] S. Ullah *et al.*, "Applications of UWB Technology", *The 5th annual International New Exploratory Technologies Conference*, pp. 225 - 232, 2010.